Anti-inflammatory properties of KLS-13019: a novel GPR55 antagonist for dorsal root ganglion and hippocampal cultures

Douglas E. Brenneman (doug@kannalife.com)
Kannalife Sciences, Inc
William A. Kinney
Kannalife Sciences, Inc
Mark E. McDonnell
Kannalife Sciences, Inc
Pingei Zhao
Temple University
Mary E Abood
Temple University
Sara Jane Ward
Temple University

Research Article

Keywords: GPR55, inflammation, lysophosphatidylinositol, chemotherapy, paclitaxel, dorsal root ganglion, hippocampus and neuropathic pain

Posted Date: May 20th, 2022

DOI: https://doi.org/10.21203/rs.3.rs-1650416/v1

Abstract

KLS-13019, a novel devised cannabinoid-like compound, was explored for anti-inflammatory actions in dorsal root ganglion cultures relevant to chemotherapy- induced peripheral neuropathy (CIPN). Time course studies with 3 mM paclitaxel indicated >1.9-fold increases in immunoreactive (IR) area for cell body GPR55 after 30 minutes as determined by high content imaging. To test for reversibility of paclitaxel-induced increases in GPR55, cultures were treated for 8 hours with paclitaxel alone and then a dose response to KLS-13019 added for another 16 hours. This: “reversal” paradigm indicated established increases in cell body GPR55 IR areas were decreased back to control levels (IC50: 0.117 nM). Because GPR55 had previously reported inflammatory actions, IL-1b and NLRP3 (inflammasome-3 marker) were also measured in the “reversal” paradigm. Significant increases in all inflammatory markers were produced after 8 hours of paclitaxel treatment alone that were reversed to control levels with KLS-13019 treatment. Accompanying studies using alamar blue indicated that decreased cellular viability produced by paclitaxel treatment was reverted back to control levels by KLS-13019. Similar studies conducted with lysophosphatidylinositol (GPR55 agonist) in DRG or hippocampal cultures demonstrated significant increases in neuritic GPR55, NLRP3 and IL-1b areas that were reversed to control levels with KLS-13019 treatment. Studies with a human GPR55-b-arrestin assay in DiscoverX cells indicated that KLS-13019 was an antagonist without agonist activity. These studies indicated that KLS-13019 has anti-inflammatory properties mediated through GPR55 antagonist actions. Together with previous studies, KLS-13019 is a potent neuroprotective, anti-inflammatory cannabinoid with therapeutic potential for high efficacy treatment of neuropathic pain.

Introduction

Neuropathic pain is a pathological condition characterized by abnormal pain sensations, including spontaneous pain, hyperalgesia and allodynia. Clinical data indicate that approximately 50% of treated individuals were unresponsive to current pharmacotherapies, and in those that receive some benefit, pain relief was typically incomplete (Bonezzi and Demartini 1999). Of particular therapeutic interest to us was neuropathic pain associated with chemotherapy-induced peripheral neuropathy (CIPN). In this adverse effect produced by many chemotherapeutic regimens, 30–40% of patients experience a progressive, enduring, and sometimes irreversible condition featuring pain, numbness, tingling and sensitivity to cold in the hands and feet (Gutierrez-Gutierrez et al 2010). Three key mechanisms have been proposed in the development of CIPN: mitochondrial dysfunction, loss of Ca + + homeostasis, and oxidative stress (Celsi et al. 2009; Han and Smith 2013; Canta et al. 2015). Associated effects on peripheral nerves can lead to oxidative stress and inflammation, sensitization and spontaneous activity of peripheral nerve fibers, and hyperexcitability in the dorsal column of the spinal cord leading to ascending pain pathway sensitization (Peters et al. 2007). Furthermore, various models of neuropathic pain have demonstrated changes in hippocampal functioning including memory deficits (Tyrtyshnaia and Manzhulo 2020) and impaired long-term potentiation (Kodama et al. 2007).

Recently there has been resurgence in interest in the potential medical utility of the Cannabis plant and its constituents, particularly in the treatment of pain. Cannabidiol (CBD) is a non-psychoactive component of *Cannabis sativa* that is neuroprotective, with reported effects on reducing pain and allodynia in various models (Milost et al. 2020). We have recently reported that CBD prevents the development of paclitaxel-induced mechanical sensitivity in mice *in vivo* (Ward et al. 2011, 2014, 2017). Additionally, we and others have demonstrated that CBD and other non-psychoactive cannabinoids are effective in animal models of spinal cord injury-associated neuropathic pain (Li et al. 2018). However, CBD has limitations in terms of potency, efficacy, safety, and oral bioavailability (Brenneman et al. 2018; Foss et al. 2021). With the recognition that optimization of CBD was warranted, the development of analogues of CBD was undertaken with the eventual emergence of KLS-13019 (Kinney et al. 2016), a novel compound that has been shown to be effective in both the prevention and reversal of allodynia in a mouse model of CIPN (Foss et al. 2021).

While a previous report indicated that both CBD and KLS-13019 were effective in preventing allodynia, only KLS-13019 was shown to be effective in reversing allodynia that was established in mice treated with paclitaxel, a chemotherapeutic agent recognized to reproducibly produce allodynia in mice. Using identical treatment paradigms, these pivotal background studies clearly indicated CBD was not effective in reversing allodynia, although morphine tested under the same conditions did result in high efficacy reversal of mechanical allodynia. Earlier mechanistic studies of effects on KLS-13019 and CBD focused on neuroprotective effects produced through mitochondrial NCX-1, a Na-Ca exchanger that regulates calcium levels important to preventing neuronal injury (Ryan et al. 2009). Pharmacological blockade and siRNA-mediated reduction of mNCX-1 were shown to effectively inhibit the neuroprotective effects of both CBD and KLS-13019 in rat dorsal root ganglion cultures (Brenneman et al. 2019). Thus, it was concluded that short-term (3–5 hour) neuroprotection from paclitaxel toxicity in DRG neurons produced by CBD and KLS-13013 was mediated through mNCX-1. However, longer term treatment with paclitaxel clearly produced an important difference in the responses between the two compounds on reversing allodynia in the mouse CIPN model. Because of the known importance of neuroinflammation in CIPN (Fumagalli et al. 2021), the focus of our studies pivoted to mediators of inflammation. As with the neuroprotective effects mediated by regulation of mNCX-1, the strategy for selecting target candidates relevant to inflammation was based on cannabidiol and endocannabinoid pharmacology (Bih et al. 2015; Guerrero-Alba et al. 2019). GPR55 has been described as an endocannabinoid GPCR associated with pain and inflammation (Staton et al. 2008). Recently, Okine et al. (2020) have demonstrated positive effects of GPR55 receptor antagonism in a rodent model of formalin-induced inflammatory pain.

Thus, with the focus of our mechanistic studies shifting to inflammation, consideration of GPR55 and the inflammasome-3 were addressed experimentally in DRG and hippocampal cultures. Previous studies had clearly shown that GPR55 played an important role in pain modulation (Schuelert and McDougall 2011, Staton et al. 2008). Previous data had suggested a proinflammatory role for GPR55 in innate immunity (Chiurchiu et al. 2015). Further, based on these previous reports and our own preliminary data which indicated that paclitaxel elicited increases in GPR55 immunoreactive area in DRG cultures, the present studies were undertaken. In addition, an emerging concept was that chemotherapeutic agents (including

paclitaxel) promote inflammatory responses through activation of the NLRP3 inflammasome (Zeng et al. 2019). Therefore, the potential role of NLRP3, a critical component of inflammasome-3, was also examined.

In the studies to be described, paclitaxel and the lysophosphatidylinositol arachidonate (LPIA), an endogenous agonist of GPR55 (Yamashita et al. 2013), were shown to produce a rapid and robust increase of GPR55 immunoreactive area in DRG cultures. These elicited increases in GPR55 were completely prevented and reversed by co-treatment with KLS-13019. Furthermore, increases in proinflammatory IL-1b and NLRP3 immunoreactive area were also responsive to KLS-13019 treatment, bringing their increased immunoreactive area levels back to that of control cultures. Together, the proposed rationale for KLS-13019 in mediating anti-inflammatory actions resides in a GPR55 antagonist outcome that can block the inflammatory actions of both paclitaxel and LPIA in rat DRG cultures.

Materials And Methods

Materials

Alamar blue and Nerve Growth Factor were obtained from Invitrogen (Eugene, OR). Paclitaxel was obtained from Teva Pharmaceuticals USA (Sellersville, PA) as a 6 mg/ml solution containing 527 mg polyoxyl 35 castor oil, 2mg citric acid and 49.7% dehydrated alcohol /ml. CY-09 (SML2465) and cannabidiol were obtained from Millipore-Sigma.

The synthesis of KLS-13019 has been described previously in detail (Kinney et al. 2016). Verification of the structural identity for KLS-13019 was determined by ^{1}H NMR, ^{13}C NMR, HMBC, HSQC, COSY, NOESY, LC/UV, and LC/MS. The purity of KLS-13019 was 98.6% as determined by LC/MS.

Culture models

Dissociated dorsal root ganglia (DRG) cultures derived from embryonic day 18 rats were employed as the primary assay system to explore anti-inflammatory mechanism of action for KLS-13019 in the context of reversing established inflammation associated with paclitaxel treatment. In brief, rat DRG were obtained commercially through Brain Bits (Springfield, IL) and cultures prepared according to methods described previously (Brenneman et al. 2019). Tissue was dissociated with a papain-based kit from Worthington Biochemical Corporation (Lakewood, NJ). The DRG cells were plated at low density (10,000 cells / well) in a 96-well format and maintained in serum-free medium consisting of Neurobasal Medium supplemented with B27, GlutaMAX (Gibco) and 25 ng/ml Nerve Growth Factor. Poly-D-lysine coated plates (BD Biosciences, Franklin Lakes, NJ) were employed for this culture system. Prior to the initiation of experiments between days 5 and 9 in vitro, a complete change of medium was performed in a working volume of 100 mL.

Anti-inflammatory actions of KLS-13019 were also studied in hippocampal cultures that were prepared by methods previously described (Brenneman et al. 2018). In brief, dissociated hippocampal cultures

derived from embryonic day 18 rats were employed as a second test system to assess responses in a central nervous system preparation that exhibited the expression of GPR55, a drug-target candidate of KLS-13019. The primary purpose of using this culture system was to measure inflammatory responses produced by lysophosphatidylinositol arachidonate (LPIA), a recognized endogenous agonist of GPR55 (Gangadharan et al. 2013). Hippocampal tissue was obtained commercially through Brain Bits (Springfield, IL). Tissue was dissociated with a papain-based kit from Worthington Biochemical Corporation (Lakewood, NJ). The hippocampal neurons were platted at low density (10,000 cell/well) in a 96-well format and maintained in serum-free medium consisting of Neurobasal Medium supplemented with B27 and GlutaMAX (Gibco). Poly-L-lysine coated plates (BD Biosciences, Franklin Lakes, NJ) were used because of the preferential adherence and survival of neurons on this matrix support. Prior to the initiation of experiments between days 11 and 21 in vitro, a complete change of medium was performed in a working volume of 100 mL.

Culture treatments and inflammation

The primary purpose of these studies was to assess two relevant culture models for their GPR55-related responses to inflammation and then to test if our novel cannabinoid (KLS-13019) had anti-inflammatory actions on cultured neurons. Of clinical relevance to neuropathic pain, DRG cultures were treated with 3 mM paclitaxel, a chemotherapeutic agent with known inflammatory properties (Staff et al. 2020). The toxic level of paclitaxel (3 mM) used for all the present studies was based on both clinically relevant serum concentrations and a previously determined toxic concentration (3 mM) that also produced increased levels of reactive oxygen species as detected with 6-chloromethyl-2',7'-dichlorodihydrofluorescein diacetate. KLS-13019 was dissolved in dimethyl sulfoxide (DMSO) to obtain a 1 mM stock solution and then serially diluted with sterile Dulbecco's phosphate buffered saline (DPBS) from Gibco (Grand Island, NY). At the highest concentration tested (1 mM), the concentration of DMSO was $\leq$ 0.1%. To study the potential effect of KLS-13019 in reversing paclitaxel-induced inflammation, DRG cultures were pretreated with either 3 mM paclitaxel or 1 nM LPIA to establish inflammatory responses with increases in IL-1b and NLRP3 immunoreactive (IR) spot area (inflammasome-3 marker) being demonstrated. After the establishment of an inflammatory response, KLS-13019 were added to the cultures for an additional 16 hours, with the paclitaxel remaining on the cultures. At the conclusion of the 16-hour treatment period, cultures were fixed and assays as described in the following immunofluorescent assay section. This sequence of 8-hour paclitaxel treatment followed by KLS-13019 treatment will be referred to as the "reversal" paradigm for DRG cultures throughout these studies.

The primary purpose of the hippocampal studies that investigated the responses produced by treatment with lysophosphatidylinositol arachidonate (LPIA), a recognized endogenous agonist of GPR55, was to elicit changes in inflammatory responses that were targets for reduction by KLS-13019. Based on preliminary experiments, it was determined that 1 nM LPIA produced the maximal increases in GPR55 after two hours of incubation. To assess hippocampal in a similar "reversal" paradigm for inflammation as that conducted for DRG, a similar but a shorter period of treatment (8-hour) was utilized. Hippocampal cultures were treated with LPIA (1nM) to establish inflammatory responses as measured

with IL-1b and NLRP3 for four hours. After sister cultures were assay for viability with alamar blue and fixed, other cultures in the same experiment were treated with KLS-13019 to test for possible reversal of the inflammatory responses during an additional four-hour treatment. This later treatment with KLS-13019 was done without the removal of the LPIA. At the conclusion of this second 4-hr treatment period, the cultures were assayed for viability and then fixed for immunofluorescence assays of inflammation-related targets.

Immunofluorescent assays

To assess the effects of various KLS-13019 treatments, immunofluorescent methods were used to measure neuronal responses in both DRG and hippocampal cultures. The goals for these assays included: 1) identification of neuronal structures with antibodies to type III beta tubulin; 2) to assess the immunoreactive spot area of selected molecular targets (IL-1b, GPR55 and NLRP3) with their respective primary antibodies and distinctively labeled secondary antibodies; and 3) to compare the relative responses of the molecular targets in both neuronal cell bodies and neurites. Prior to fixation, growth medium was removed and the wells were rinsed one time with 100 mL DPBS (37^{o} C). This warm rinse is particularly important to maintain structural stability of neurites. After removal of the DPBS, cultures were fixed for 20 min at room temperature with 50 mL / well of 3.5% formaldehyde (Sigma-Aldrich: 252549) in warm (37^{0}C) DPBS that contained 5.5 mg/mL of Hoechst 33342 dye (Invitrogen: H3570) to label cell nuclei. After removal of the fixative, the cultures were rinsed twice with 100 mL of DPBS and then a permeabilization - blocking buffer containing 5% normal goat serum and 0.3% triton-X100 in DPBS was added to the cultures for 10 min. After removal of the blocking buffer, the cultures were rinsed twice with 100 mL of DPBS and then primary antibodies were added for one-hour incubation at room temperature. Neurons were identified with antiserum to type III beta tubulin (tuj 1) to measure changes in all neuronal structure parameters. The primary antiserum employed was a rabbit polyclonal obtained from Sigma –Aldrich (T2200) and used at 1:250 dilution. The secondary antibody was an Alexa Fluor 488-conjugated Fab fragment of goat anti-rabbit IgG obtained from Life Technologies (A11070) used at 1:600 for 30 minutes. After the secondary antibody treatment, cultures were rinsed 3 times with 100 mL of DPBS before performing high content fluorescent analysis. For storage, the wells were placed in 100 mL of sterile DPBS, with the plates wrapped in aluminum foil and maintained at 4^{0} C. For the detection of inflammatory markers, the following primary antibodies were used: IL-1b (PA5-88078); NLRP3 (PA5-79740); and for GPR55 (ab203663). All primary antibodies for IL-1b and NLRP3 were obtained from Life Technologies. The GPR55 antibody was obtained from Abcam. All primary antibodies were diluted 1:250 and all secondary antibodies were used at 1:600. The secondary antibodies were obtained from Life Technologies. The following Alexa Fluor dyes labeled the secondary antibodies: Alexa Fluor 488 (A11070), 555 (A32732), 687(A32733) and 750 nm (A21039). By using secondary antibodies with differing dyes, the same culture wells were assayed for multiple molecular targets.

High content image analysis

The immunofluorescent assays were conducted on the Cell Insight CX5 high content imaging system (Thermo Fisher Scientific). The system is based on an inverted microscope that automatically focuses and scans fields of individual culture wells using a motorized stage at predetermined field locations. Fluorescent images from individual fields (895mm x 895mm) were obtained with a 10 x (0.30NA) Olympus objective and Photometrics X1 CCD camera, with analysis by HCS Studio 2.0 Software. The light source was LED with solid state five-color light engine used with filter sets that had the following excitation/emission: 386/440, 485/521, 560/607, 650/694 and 740/809). With this capability, multiple fluorescent assays in a single well were conducted. Images were acquired in a low-resolution mode (4 x 4 binning). Image analyses for neuronal cell bodies and neurites were performed with the Cellomics Neuronal Profiling BioApplication. For analysis of neurons, objects were identified as cells if they had valid nuclei and cell body measures based on size, shape and average intensity. Acceptable ranges were determined in preliminary studies to ensure that aggregated cells and non-cellular objects were excluded from the analysis.

For both the DRG and hippocampal cultures, the goals were to examine the immunoreactive spot areas for all the analytes of neurons only. Because the neuronal morphology was different between the two cultures, unique size and shape parameters for cell bodies and neuritic arbors were empirically determined for each culture type in preliminary studies. Once these parameters were determined, the analyses for each culture type were used throughout their respective experiments. Important to these analyses, an essential goal was to compare the immunoreactive spot areas for all analytes in both cell bodies and neurites. Type III beta tubulin immunoreactivity was used to identify the neurons for each culture type (Brenneman et al. 2019). For DRG cultures, twenty predetermined fields of view were sampled in each of six replicate wells per plate, with two replicate plates from different cellular preparations used for each assay. This extensive sampling of the low-density cultures was conducted as some fields contained 1-3 neurons while other fields contained complex networks of 10 or more neurons. The age of the DRG cultures at the time of analysis was 8-10 days after plating. Because primary cultures exhibit a variety of neuronal phenotypes and a range of morphological complexities, extensive sampling was employed to obtain an average neuronal response with the inflammatory markers. For measuring parameters of type III beta tubulin immunoreactivity and spot analysis for the inflammatory markers, the Cellomics Neuronal Profiling Bioapplication was used that combined spot analysis on neurons that resided within this bioapplication. For analysis of spot immunoreactivity with this bioapplication, a key parameter was the empirical establishment of fluorescent thresholding that permitted the use of a dynamic range that optimized the measurement of fluorescent differences among the treatment groups as well as distinguishing the fluorescent signal from background. This thresholding level was set based on our previous experience with antibody-based assays and the smallest distinguishable size of immunoreactive spots (radius:1.5 m) under our imaging conditions. With this algorithm, the immunoreactive area was a relative measure that was characterized by an effective computerized spot analysis in a rapid screening mode. Importantly, the same imaging parameters for neurons from all treatment groups were employed for the DRG studies. The key comparisons in these studies were aimed at measuring the changes in immunoreactive area that was associated with KLS-

13019 treatment. Due to the observed differences in the cellular distribution among the analytes, the cellular locations of all inflammatory markers in DRG were determined, thus distinguishing the relative changes between cell bodies and neurites. This capability and experimental focus were obligatory aspects of measuring the inflammatory markers by image analysis. Because dissociated hippocampal cultures exhibited more abundant neurons and had more extensive neuritic arbor than the DRG cultures, ten predetermined fields of view were sampled in each of six to eight replicate wells per plate, with two replicate plates from different cellular preparations used for each assay. The fluorescent thresholding parameters for the immunoreactive spot analysis for hippocampal cultures were similar to that employed for the DRG cultures. Again, the goal of the studies was to obtain measures of the relative changes in immunoreactive area for each of the analytes after KLS-13019 treatment. In contrast to the DRG cultures, the experiment with hippocampal cultures were conducted 14-20 days after plating. As in the case of DRG cultures, field sampling was extensive in order to obtain an assessment of the average neuronal response to the pharmacological treatments. For each experiment, the values are the mean from 6 wells with 10 fields per well being analyzed. An estimate of 400-600 neurons were assessed for each treatment. In all cases, the results were expressed as immunoreactive area of each of the analytes per neuron.

Since CBD had played a prominent role in the discovery and mechanistic history of KLS-13019, preliminary studies also were conducted in hippocampal cultures to investigate the possible activity of this cannabinoid on GPR55 immunoreactive area after treatment with 1nM LPIA. Treatment with 10 mM CBD for 6 hours has no detectable effect on LIPA-induced increases in GPR55 IR area in either neurites or cell bodies of hippocampal neurons (data not shown). Furthermore, CBD treatment produced only low efficacy protection (40% of maximum) from LPIA-mediated decreases in cellular viability as assessed by the alamar blue assay. Since these screening studies with CBD and GPR55 were ineffective, further studies in DRG cultures were not performed.

Mitochondrial GPR55 localization

Exploratory studies were conducted on day 21 hippocampal cultures to assess the possible localization of GPR55 within some mitochondria. These studies were undertaken because of the central importance of GPR55 in the inflammatory responses reported in the present study as well as our findings that both DRG and hippocampal cultures respond to increases produced by the GPR55 agonist: LPIA. The primary antibody used as a marker for mitochondria was GT6310 for cytochrome c oxidase 4 [COX4] (Life Technologies). GT6310, used at 1:300, is a mouse monoclonal antibody that was made to a recombinant fragment between amino acid 1-169 in COX4. The secondary antibody (A-21037) for the COX4 assay was goat anti-mouse labeled with Alexa Fluor 750 (Life Technologies) that was used at 1:1000. For measuring parameters of type III beta tubulin immunoreactivity and spot analysis for COX4, the Cellomics Neuronal Profiling Bioapplication was used that combined spot analysis on neurons that resided within this bioapplication. Conditions for detecting neurons and GPR55 were identical to that described previously. For analysis of spot immunoreactivity with this bioapplication, a key parameter was the empirical establishment of fluorescent thresholding which was based on our previous experience with

antibody-based assays and the size of the spots which were set at the lowest limit for spot radius (1.5 m). Under these imaging parameters, the spot overlap function was set a 100% in order to detect spot overlap with the highest stringency. The goal of these studies was to use the highest exclusionary conditions to estimate if such colocalizations may exist within in the limits of detection for this system. With the use of pseudo color imaging, 100 % overlapped spots were reported with a blue color, while COX4-positive spots alone were reported as yellow and GPR55-positive spots alone were reported red.

Viability assay

At the conclusion of some experiments, sister cultures to those assessed by image analysis were evaluated first with the viability dye alamar blue. Because of our interest in mitochondria, we noted with interest the suggestion (Iuchi et al. 2019) that the alamar blue dye “mainly” consisted of an assessment of succinate dehydrogenase reductive activity, an enzyme that participates in both the electron transport chain and the citric acid cycle. The preferred dye was alamar blue as this assay was conducted first and then the dye washed off the cultures for subsequent fixation and follow-up immunocytochemical assays. On every plate, wells without cells were used to provide a blank reading that was used to subtract background fluorescence. For the alamar blue viability assay, 10 ul of the dye was added directly to the culture well that contained 100 ul of nutrient medium. Incubation times with the dye ranged from 2-4 hours. Fluorescence was measured at an excitation of 530nm and an emission of 590 on a Cytofluor plate reader.

β-arrestin assay

A commercial assay for b-arrestin was obtained from Eurofins that provided a means of testing human GPR55 in a cell line (93-024C2) that had a background of CHO-K1. In this assay, agonist-induced activation of GPR55 stimulated binding of b-arrestin to the Pro-Link-tagged GPCR and forces complementation of two enzyme fragments that resulted in the formation of an active b-galactosidase enzyme. The Pro-Link fragment of b-gal was a low affinity enzyme donor that was stably expressed with b-Arrestin tagged with an enzyme acceptor. This interaction leads to an increase in enzyme activity that was measured using chemiluminescent PathHunter detection reagents. For our application, the GPR55 agonist lysophosphatidylinositol (LPI) was tested from 0.1 nM to 30 mM to increase the relative luminescent signal relative to that of control. Incubations were conducted for 90 min at 37 degrees C in 5% CO2. Lysophosphatidylinositol (LPI) produced a robust and reproducible signal at 10 mM in this transfected system. For the GPR55 antagonism assay, KLS-13019 concentrations ranging from 0.1 nM to 30 mM were pre-incubated with the cells for 10 min prior to the addition of 16 mM LPI. Concentrations of KLS-13019 ranging from 0.1 nM to 30 mM were tested alone for possible effects of agonistic activity on b-arrestin. The data indicated that KLS-13019 had no detectible agonist activity in the b-arrestin assay.

Statistical Analysis

All statistical comparisons were made by ANOVA, with normality of values tested by the Shapiro-Wilk test followed by a multiple comparison of means test with the Holm-Sidak method as performed through Sigma plot 14. All EC50 and IC50 values were generated by the curve-fitting procedure provided by the 4-parameter logistic analysis.

Results

The goals of these studies included an exploration of a potentially novel mediator (GPR55) of inflammatory responses to paclitaxel treatment of dorsal root ganglion cultures and the testing of our lead **compound** (KLS-13019) for anti-inflammatory actions. Since the initial interest was to establish an association of a chemotherapeutic agent (paclitaxel) with inflammation, a time course of changes in the immunoreactive (IR) area of a putative proinflammatory target (GPR55) was measured in dorsal root ganglion cultures after treatment with paclitaxel. In **figure 1a**, a comparison of GPR55 IR area was made in cell bodies and neurites as measured by high content imaging in neurons that were identified with antibodies to Type III beta tubulin. These initial studies indicated that significant increases in GPR55 IR area were apparent in the cell bodies after 15 minutes of incubation and plateauing after 30 minutes ($p < 0.01$). The paclitaxel-induced increases in cell bodies were 1.9-fold greater than that observed in control cultures. No further increases in cell body GPR55 were observed up to 8 hours of incubation. In contrast, the area of GPR55 in neurites after treatment with 3 mM paclitaxel remained unchanged throughout the 8-hour time course. While these effects of paclitaxel were relevant to our interest to chemotherapy-induced peripheral neuropathy (CIPN), further exploration of GPR55 responses were conducted with a recognized agonist (Gangadharan et al. 2013) of GPR55: lysophosphatidylinositol arachidonate (LIPA). Based on preliminary experiments of concentration-effect responses of LIPA to determine maximally effective conditions, a time course of 1nM LIPA on GPR55 IR area was conducted with the rat DRG cultures. As shown in **Figure 1b**, significant increases in GPR55 IR area were observed in neurites after 30 minutes of incubation, with an apparent plateau in the response observed between 30 minutes and 8 hours of incubation. The LPIA-induced increases in neuritic GPR55 were 40% greater than that of control cultures. In contrast to the responses of paclitaxel shown in figure 1a, 1nM LPIA produced no significant increases in GPR55 IR area in the cell bodies of the DRG during the 8- hour time course. While the time course of both paclitaxel and LPIA produced significant changes in GPR55 in the DRG neurons, the responses between cell bodies and neurites were consistently different between these two regions of the neurons that was dependent on the nature of the compound used to elicit the GPR55 increases. In addition, the. magnitude of the GPR55 IR area response in cell bodies after paclitaxel was much greater (1.9-fold) than that observed in the neurites after LPIA treatment (40%). Although the cellular responses between the two agents were different, the conditions of image analysis parameters involving cell body and neurite demarcations for DRG neurons were the same between the two series of time courses. Together, these data indicated that significant increases in GPR55 IR area were rapidly produced (30 minutes) in DRG neurons after treatment with either a GPR55 agonist or the chemotherapeutic agent paclitaxel.

A second major goal of these studies was to test if changes in GPR55 IR area were reversible after treatment with KLS-13019, a novel compound that has been shown to reverse mechanical allodynia in paclitaxel-treated mice (Foss et al. 2021). To test for reversibility of paclitaxel-induced increases in cell body GPR55 IR area, DRG cultures were pre-treated for 8 hours with 3 mM paclitaxel and then the cultures were co-treated for an additional 16 hours with various concentration of KLS-13019 in the continuing presence of paclitaxel. As shown in **Figure 2a**, treatment with KLS-13019 for 16 hours produced a concentration-dependent decrease in GPR55 cell body area back to control levels. The IC50 for this effect was shown to be 117 $\pm$ 56 pM. In addition, the effect of the 8-hour pretreatment with paclitaxel alone is shown with the reference line for GPR55 IR area in cell bodies. These studies indicated that a complete reversal of the increases in GPR55 IR area were demonstrated with KLS-13019 treatment. While the demonstration of reversibility of the increased GPR55 was of significance, cell viability also was measured in cultures from these experiments as shown in **Figure 2b**. Using the same treatment paradigm as that for the GPR55 responses, KLS-13019 treatment was shown to reverse back to control levels the paclitaxel-induced decreases in cell viability as measured with alamar blue. Thus, paclitaxel treatment alone for 8 hours produced a 40% decrease in cellular viability in the DRG cultures that could be restored to control levels by 16-hour treatment with KLS-13019 with an EC50 of 200 $\pm$ 46 pM.

To address the possibility that proinflammatory markers may be playing a role in the responses of DRG cultures to paclitaxel and LPIA, additional analytes for IR area for IL-1b (proinflammatory cytokine) and NLRP3 (inflammasome -3 component) were conducted. As shown in **Figure 3a**, the time course of paclitaxel effects on IL-1b and NLRP3 IR area in cell bodies were compared. For IL-1b IR area (closed circles), significant ($P < 0.05$) increases were observed after 15 min of 3 mM paclitaxel treatment that reached an observed peak at 30 minutes. The amount of increase in IL-1b was 74 % over that observed at the beginning of the incubation. Similarly, paclitaxel-induced increases in NLRP3 IR area (open circles) were also observed after 30 minutes of treatment ($P < 0.001$). The observed maximum effect (29% increase above control) for NLRP3 IR area was observed after 30 minutes of paclitaxel treatment. Thus, a similar time course was observed in DRG neurons after paclitaxel-induced increases in these two proinflammatory markers.

As a follow-up analysis to the effect of the GPR55 agonist (LPIA), IL-b and NLRP3 were measured in neurites after 1 nM LPIA treatment of DRG cultures. As shown in **Figure 3b**, treatment with LPIA produced significant increases in neuritic IL-1b after 15 minutes of incubation ($P < 0.017$). Longer duration of treatment with LPIA did produce further increases in IL-1b to a peak at one hour with significant decreases observed after 2 hours of treatment. Similarly, LPIA (1nM) produced increases in neuritic NLRP3 that peaked at 30 minutes, with more prolonged incubation producing an attenuation of observed increases produced by LPIA. Thus, both paclitaxel and LPIA had effects on both these pro-inflammatory markers, although the cellular location of these increases was different for the predominant effects between the two compounds and the transient nature of the increases were apparent with LPIA, but not paclitaxel.

Like the studies on GPR55, exploration of the anti-inflammatory actions of KLS-13019 was continued by measuring the effect of this compound on IR areas of both IL-1b and NLRP3 utilizing the “reversal paradigm for DRG cultures. In this series of experiments, cultures were pre-incubated with 3 mM paclitaxel for 8 hours after which the changes in inflammatory marker IR areas were measured. As shown by the 8-hour dotted reference line of paclitaxel treatment alone in figure 4A, a significant increase in IL-1b was detected in the cell bodies of DRG neurons. With the reversal paradigm employed, treatment with KLS-13019 was initiated in cultures that had already been treated for 8 hours with paclitaxel. The duration of the KLS-13019 treatment was for 16 hours without removing the paclitaxel. The goal of this experiment was to test if a previously established inflammatory response from IL-1b could be returned to control levels with the KLS-13019 treatment, without removing the paclitaxel. As shown in **figure 4a**, a concentration-dependent decrease in IL-1b was observed in cell bodies, with an IC50 of 156 $\pm$ 45 pM. At concentration of 1 nM KLS-13019, the mean level of IL-1b was not different from that of the control value in cell bodies. Similar studies KLS-13019-mediated reversal studies also were conducted by measuring NLRP3 as shown in **Figure 4b**. As with IL-1b, the 16 hours treatment with KLS-13019 resulted in a concentration-dependent decrease in paclitaxel-induced increases in NLRP3 with an IC50 (140 $\pm$ 72 pM), similar to that measured with IL-1b. Together, these studies support the conclusion that KLS-13019 reversibly intervened in an established inflammatory response in cultured DRG neurons previously treated with paclitaxel during a 24-hour test period.

GPR55 and Hippocampal cultures

To further explore GPR55-mediated responses, a series of experiments were conducted in dissociated hippocampal cultures, with a particular interest in the reversibility of LPIA-mediated changes in a CNS preparation that is recognized to express GPR55. Utilizing a similar, but shorter (8-hr) duration of treatment schedules, LPIA was used to a elicit potential effects on GPR55 expression as well as inflammatory markers. For the hippocampal experiments, 1 nM LPIA was added to the cultures alone for 4 hours and then various concentrations of KLS-13019 were added to the cultures without removing the LPIA. As shown from the reference lines in **figure 5a**, treatment with LPIA (1nM) alone produced a doubling of the GP55 IR area in neurons of hippocampal neurons after 4 hours. Co-treatment with of KLS-13019 and 1nM LPIA produced a concentration-dependent decrease in neuritic GPR55 IR area back to control levels (IC50:107 $\pm$ 19 pM). In the same cultures, neuritic NLRP3 immunoreactive (IR) areas were measured as shown in **figure 5b**. Similar to that observed from GPR55, concentration-dependent decreases in neuritic NLRP3 were observed after treatment with KLS-13019 (IC50: 129 pM $\pm$ 43 pM). These studies again indicated that co-treatment with of KLS-13019 and 1nM LPIA produced decrease in neuritic NLRP3 IR area back to control levels. As shown in **Figure 5c**, KLS-13019 treatment in this reversal paradigm produced decreases in neuritic IL-1b area values back to control levels that had been elevated by pre-treatment with 1 nM LPIA for 4 hours on hippocampal cultures (IC50: 208 $\pm$ 35 pM). Within the same experimental treatment schedule, decreases in the viability as measured with the alamar blue assay after LIPA treatment were reversed by KLS-13019 treatment (EC50: 94 $\pm$ 22 pM) as shown in **Figure 5d**. Together, the studies conducted in hippocampal neurons produced similar responses on GPR55 and inflammatory responses to that observed on neurons in DRG cultures. Importantly, KLS-13019 exhibited

high potency, high efficacy anti-inflammatory actions in hippocampal cultures in addition to the observed effects on sensory neurons from DRG.

To further explore the potential role of the NLRP3 inflammasome-3 in LPIA-related in hippocampal cultures, an inhibitor (CY-09) for the assembly of the inflammasome-3 complex was tested for ability to block LPIA-mediated increases in NLRP3 during a 6-hour test period. Utilizing high content imaging, the increase in IR area of NLRP3 in neurites elicited by 1 nM LPIA was completely blocked by pretreatment with 10 mM CY-09 as shown in **figure 6a**. In addition, the control levels of NLRP3 were not affected by CY-09 treatment alone. In the same cultures assayed for NLRP3 spot area, cell viability was measured prior to fixation to monitor possible outcomes as assessed with the alamar blue assay. As shown in **Figure 6b**, treatment with 1nM LPIA alone for six hours resulted in a decrease to 58% of control values in the viability assay. Importantly, pretreatment of hippocampal cultures with CY-09 prevented the loss of cellular viability produced by 1 nM LPIA. Together, these studies indicate that an inhibitor of inflammasome assembly (CY-09) can effectively block LPIA-mediated effects on increases in neuritic NLRP3 area and decreases in LPIA-mediated cellular viability. Because LIPA is a potent agonist of GPR55, these studies suggest that this orphan GPCR is proinflammatory with a capability of producing reversable decreases in both cellular viability and neuroinflammation.

To provide further evidence of KLS-13019 as a GPR55 antagonist, additional studies were conducted with a DiscoverX assay system with human GPR55 from which increases in b-arrestin produced by 16 mM LPI were completely blocked by 30 mM KLS-13019 (open triangles) in this model system (**Figure 7**). In addition, as shown in the open circles, treatment with KLS-13019 alone produced no increases in b-arrestin, consistent with this compound having no agonist activity on human GPR55 in this model system. As a positive control, ML-193, a recognized high potency GPR55 antagonist, also blocked LPI-mediated increases in b-arrestin, consistent with this compound being a GPR55 antagonist.

Based on reports that mitochondria can co-localize with the NRLP3 inflammasome (Kelly et al, 2019), three-week-old hippocampal cultures were analyzed by high content imaging for the presence of GPR55 IR spot area and COX4 IR spot area in Type III beta tubulin-positive neurons. A spot co-localization algorithm within a neuronal profiling bioapplication was used to screen spots for GPR55 and COX4 that were 100% overlapping. Identification of such co-localized spots were displayed utilizing pseudo color blue, with spots showing less than 100% overlap being displayed in red for GPR55 and yellow for COX4. A prominent area spot overlap of GPR55 and COX4 on a proximal neurite is highlighted in the left panel of **Figure 8**. These data suggested that within the measurement limitations of these two IR spots of $\leq$ 1.5 m radii, complete overlap could be detected. These data are consistent with the conclusion that GPR55 can be localized to mitochondria in a sub-population hippocampal neurons.

Discussion

The precedent finding which led to the present studies was that treatment with KLS-13019, a novel cannabinoid, produced a complete reversal of mechanical allodynia in a mouse model of paclitaxel-

induced peripheral neuropathy. This mouse model of CIPN employed chronic paclitaxel treatment for one week followed by the demonstration of mechanical allodynia after 11 days. A reversal paradigm used a 3-day treatment schedule with orally administered KLS-13019 followed by an assessment of mechanical allodynia again that was compared to pre-paclitaxel responses. This reversal finding was characterized by its dose-dependency that was complete in its efficacy in comparison to control responses. Since this response to chronic treatment was so robust and complete, a consideration of another contributing mechanism besides mitochondrial NCX-1 (Brenneman et al., 2019) was undertaken in the dissociated DRG cultures, as the neuroprotective action of NCX-1 against paclitaxel toxicity previously reported was discovered under only acute (3-5 hours) treatment conditions in which both KLS-13019 and CBD were equally efficacious and mechanistically dependent on NCX-1.

Because of the recognized complexity of CIPN involving both acute (hourly) and chronic (daily and weekly) components, an additional mechanism for KLS-13019 was explored that was based on three findings from the literature: 1) the emerging preclinical studies which suggested that neuroinflammation may be playing important roles in CIPN (Fumagalli et al. 2021); 2) evidence that an atypical cannabinoid receptor (GPR55) has a role in mediating neuropathic pain in a mouse model of CIPN (Staton et al. 2008); and 3) GPR55 receptor antagonism recently being reported to have positive effects in a rodent model of formalin-induced inflammatory pain (Okine et al. 2020).

Our investigation of GPR55 began with exploration of paclitaxel-induced changes in GPR55 immunoreactive area in dissociated DRG neurons as shown in the time course of Figure 1a. Since this analysis was conducted with high content imaging, it was possible to distinguish between increases that were detected in cell bodies and those that occurred in neurites of DRG cultures. These studies indicated that this putative proinflammatory GPCR was increased within 15-30 minutes of treatment with a clinically relevant amount (3 mM) of paclitaxel. The concept that emerged from this finding is that GPR55 may be among multiple sentinel mechanisms that are induced after exposure to pro-inflammatory drugs or endogenous agonists. Subsequent studies with one of these GPR55 agonists (lysophosphatidylinositol arachidonate [LPIA]) also produced an increase in GPR55, but the cellular localization of the elevations of this receptor were in the neurites, with no apparent increases observed in the cell bodies. While the reason for this GPR55 localization difference between paclitaxel and LPIA is not yet apparent, it is possible that multiple or different processes could be elicited by the two substances. For example, it is known that paclitaxel inhibits antegrade axonal transport (LaPointe et al. 2013) and such an inhibition could slow the transport of induced GPR55 from the cell bodies to the neurites. In addition, the antegrade velocity of mitochondrial transport are significantly decreased by paclitaxel in a concentration-dependent process (Smith et al. 2016). Alternatively, because paclitaxel has been shown to mediate priming of the NLRP3 inflammasome activation through TLR4 (toll-like receptor-4) receptors in bone marrow-derived macrophages (Son et al. 2019), it cannot be excluded that multiple receptors could be involved in explaining differential cellular location of IL-1b and NLRP3 increases after paclitaxel treatment. Although the mechanism(s) of receptor induction and receptor complexity/specificity remain to be established, these data clearly show that GPR55 is rapidly and potently inducible in DRG neurons by multiple substances. Of importance to a potential interaction with KLS-13019 is the observation that the

induced increases GPR55 produced by paclitaxel could be prevented by this drug candidate as well as increases produced by LPIA in DRG neurites. This confluence of reversable actions produced by KLS-13019 may have a common origin: GPR55 antagonism by the drug candidate, although it is not known if paclitaxel has either a direct or indirect action at GPR55. This mechanism for KLS-13019 was further supported by the demonstrated GPR55 antagonism action in the b-arrestin effects shown in figure 7.

The observation of the present study wherein an endogenous agonist and a drug can increase the expression of a GPCR is an atypical, albeit a defining response. Plasma membrane GPCRs most often either remain either unchanged in receptor density or are down-regulated after prolonged treatment with their agonist (Rajagopal and Shenoy 2018). In the present study, within 30 minutes both a GPR55 agonist and a chemotherapeutic drug both produced increases in GPR55. The present findings were characterized by several observations: 1) evidence was presented that GPR55 could be detected in neurites and cell bodies of hippocampal and DRG neurons; 2) GPR55 could be detected in mitochondria; and 3) a subpopulation of GPR55 immunoreactive spots could be co-localized with mitochondria as determined within resolution limits by high content imaging of COX4 (a mitochondrial marker) and GPR55 in hippocampal neurons. While reports of other mitochondrial GPCRs have begun to appear, this remains an emerging area of pharmacology (Nezhady et al., 2020). Of potential pertinence to the present study, CB1 is among the GPCRs that have been reported in mitochondria. Further, mitochondrial CB1 has been shown to be upregulated after traumatic brain injury, indicating that the expression of this cannabinoid receptor can also undergo an upregulation in response to a pathological stress (Xu et al., 2016). Of further interest, b-arrestin, a recognized mediator of GPR55 signal transduction, has been shown to be localized on and within neuronal mitochondria (Suofu et al. 2017). Together, our data suggest that the mitochondrial GPR55 is both a target of paclitaxel in DRG neurons and perhaps a physiological mediator of inflammation in both hippocampal and DRG neurons that would be predicted to enhance the sentinel function for inflammation by producing an induction of the GPR55 receptor density. With the sentinel function as a working hypothesis, an upregulation of GPR55 may act as an amplification mechanism to further an inflammatory response, regardless if paclitaxel interactions are either directly or indirectly associated with this GPCR. In general, the present example may be suggestive of a broader concept that the location of a GPCR within an organelle has significant implications for differential pathophysiological functions distinct from that of homologous receptors located at the plasma membrane.

With a goal of linking the observed action of paclitaxel and LPIA to proinflammatory effectors, measurements of Il-1b and NLRP3 were measured in the DRG cultures. Cytokines have been associated with inflammatory pain and both are recognized mediators of CIPN in animal models (Staff et al., 2020). Of interest, a recent report has shown that LPI also can induce the secretion of the proinflammatory cytokines (IL-6 and TNF-a) from macrophages (Kurano et al., 2021). In the present study, the time course of paclitaxel-mediated increases of two mediators of inflammation (NLRP3 and IL-1b) and that of LPIA-mediated increases were similar, regardless of their localization in the neurons. While the sources of the inflammatory marker increases were presumed to be attributed to neuronal biosynthesis and processing, a contribution by non-neuronal cells also needs to explored. The action of KLS-13019 in regulating IL-

1b and NLRP3 in the reversal experiments depicted in figure 4ab, indicated a reversion back to control levels within 16 hours of KLS-13019 treatment. The fact that KLS-13019-mediated effects on cellular viability was also observed within this reversal paradigm, indicated that a protective role was also produced (Figure 2b). Together, these data are consistent with a KLS-13019-mediated effects on recognized proinflammatory and pain mediators that can be detected in DRG neurons that may be consistent with a return to pre-paclitaxel homeostasis.

An emerging concept is that chemotherapeutic agents (including paclitaxel) promote inflammatory responses through activation of the NLRP3 inflammasome (Zeng et al. 2019; Son al. 2019). Although paclitaxel is believed to be among the substances that can drive “priming” for signal-mediated events needed for the activation of inflammasome-mediated assembly in macrophages, our findings indicate that this action of paclitaxel may be similar in DRG neurons. Importantly, a novel finding of the present disclosure is that paclitaxel treatment can also increase the expression of GPR55 in DRG cultures. Thus, an alternative explanation for paclitaxel-mediated “priming” is herein described: the concept is that GPR55 is a mediator of paclitaxel-induced “priming” of NLRP3 inflammasome assembly. With this finding, GPR55 is a “priming” signal for inflammasome assembly. Our new data suggest that GPR55 is a sufficient, although not likely exclusive, priming signal in DRG cultures to mediate all of the increases in IL-1b, which is known to be elevated through the action of the NLRP3 inflammasome-3. Because paclitaxel can also produce toxic increases in mitochondrial calcium and elevated reactive oxygen species in sensory neurons, we have concluded that these actions of paclitaxel on the activation of the inflammasome complex are major actions produced by paclitaxel in sensory neurons. Thus, two roles of paclitaxel have been revealed in DRG neurons: 1) increases in the expression of GPR55; and 2) increases ROS and calcium in the mitochondria (Canta et al., 2015). The rationale for KLS-13019 mediating anti-inflammatory actions produced by paclitaxel is that this agent is an GPR55 antagonist that can block the GPR55-mediated “priming” of NLRP3 inflammasome assembly. In the present disclosure, the KLS-13019-mediated antagonism of GPR55 actions is supported through effects observed on decreasing levels of IL-1b and NLRP3 in DRG neurons. The present disclosure presents evidence that KLS-13019 is completely effective in reducing paclitaxel- and LPIA-mediated increases in these inflammatory markers back to that of control levels.

As a result of the recognized importance of sensory neurons in DRG to transmitting peripheral nociception (Krames 2014) and the reported accumulation of paclitaxel and mitochondrial reactive oxygen species in DRG from models of CIPN (Duggett et al. 2016), the preparation of choice for the in vitro studies to study protection and anti-inflammation was dissociated cultures from rat DRG. Inclusion of studies on hippocampal cultures were intended primarily to explore the scope of the anti-inflammatory actions of KLS-13019 in CNS-related neurons as well. However, KLS-13019 may have important therapeutic actions relevant to neuropathic pain in the hippocampus as suggested by previously recognized impairment of hippocampal functioning in animal models of peripheral nerve injury and neuropathic pain (Kodama et al. 2007; Tyrtyshnaia and Manzhulo 2020). Of particular relevance, hippocampal cultures also express both mNCX-1 and GPR55, the two KLS-13019-related drug target candidates that mediate protection and anti-inflammatory responses, respectively. In this present study,

the effects of LPIA on increases GPR55 immunoreactive area and elevations of NLRP3 and IL-1b were also observed in hippocampal cultures. Importantly, similar to the findings obtained in DRG cultures, KLS-13019 was able to both prevent and reverse the effects produced by LPIA in hippocampal neurons. Furthermore, the importance of the inflammasome-3 was extended with the hippocampal cultures to demonstrated that the effects on LPIA-mediated increases in NLRP3 spots area in neurons was prevented with a recognized inhibitor (CY09) of inflammasome-3 assembly (Jiang et al., 2017). In addition, the decreases in cellular viability produced by LPIA were shown to be prevented by pre-treatment with CY09, suggesting the importance of the inflammasome in producing decreases in GPR55-meidated decreases in cellular viability (see Figure 6b). Together, these studies suggest a sentinel function for GPR55 in both DRG and hippocampal neurons, extending the importance of this receptor as an early warning mechanism of some inflammatory mediators.

These studies support a pro-nociceptive, pro-inflammatory role for GPR55 that mediate acute and chronic effects in DRG. The GPR55 target is believed to be complementary to our previous studies with the NCX-1 target which exhibited acute regulation of mitochondrial calcium levels by extrusion of excess calcium in DRG (Brenneman et al. 2019). Our data suggest a bimodal pharmacological effect of KLS-13019 that can be both increase viability of sensory neurons exposed to paclitaxel and antagonize GPR55 that can mediate neuroinflammatory and sensory neuron damage that may contribute to neuropathic pain.

Declarations

Conflict of interest: Douglas Brenneman, William Kinney and Mark McDonnell are inventors of KLS-13019 and hold international patents on the technology described.

Ethics approval and consent to participants: No animal or human subject data were in this work. Animal tissues for primary cultures were purchased from a commercial source.

Informed consent: No human subjects were in these studies.

Data availability statement: Data analyzed in these studies are available from the corresponding author upon reasonable request.

Funding: These studies were supported by Grants from the National Institute on Drug Abuse (R41DA044898); (5P30DA013429-20); (RO1DA045698) and the National Institute of Neurological Disorders and Stroke (R42NS120548) of the National Institutes of Health.

Author contributions: Douglas Brenneman designed and conducted all experiments using primary neuronal cultures and wrote the draft of the manuscript. William Kinney and Mark McDonnell chemically designed and provided the purified, structurally verified KLS-13019. Pingei Zhao conducted the b-arrestin assays and authored figure 7. Mary Abood provided intellectual input on GPR55 and second messenger systems relevant to study design. Sara Jane Ward provided intellectual input on study design pertaining

to inflammation. Editing contributions were made by Brenneman, McDonnell and Ward. All authors read and approved the final manuscript.

References

1. Bih CI, Chen T, Nunn AVW, Bazelot M, Dallas M, Whalley BJ (2015) Molecular targets of cannabidiol in neurological disorders. Neurotherap 12: 699–730.
2. Bonezzi C, Demartini L (1999) Treatment options in postherpetic neuralgia. Acta Neurol Scand 100(s173):25–35.
3. Brenneman DE, Petkanas D, Kinney (2018) Pharmacological comparisons between cannabidiol and KLS-13019. J Mol Neurosci 66:121–134.
4. Brenneman DE, Kinney WA, Ward SJ (2019) Knockdown siRNA targeting the mitochondrial sodium-channel WA exchanger-1 inhibits the protective effects of two cannabinoids against acute paclitaxel toxicity. J Mol Neurosci 68:603–619.
5. Canta A, Pozzi E, Carozzi VA (2015) Mitochondrial dysfunction in chemotherapy-induced peripheral neuropathy (CIPN). Toxics 3: 198–223; doi: 10.3390/toxics3020198.
6. Celsi F, Pizzo P, Brini M, Leo S, Fotino C, Pinton P, Rissuto (2009) Mitochondria, calcium and cell death: a deadly triad in neurodegeneration. Bioch. Biophys Acta 1787:335–344.
7. ChiurchiuG V, Lanuti M, De Bardi M, Battistini L, Maccarrone M. (2015) The differential characterization of GPR55 receptor in human peripheral blood reveals a distinctive expression in monocytes and NK cells and a proinflammatory role in these innate cells. Int Immunol 27:153–160.
8. Duggett NA, Griffiths LA, McKenna OE, de Santis V, et al. (2016) Oxidative stress in the development, maintenance and resolution of paclitaxel-induced painful neuropathy. Neurosci 333:13–26.
9. Foss JD, Farkas DJ, Huynh LM, Kinney WA, Brenneman DE, Ward SJ (2021) Behavioral and pharmacological effects of cannabidiol (CBD) and the CBD analogue KLS-13019 in mouse models of pain and reinforcement. Brit J Pharmacol 178:3067–3078.
10. Fumagalli G, Monza L, Cavaletti G, Rigoli o R, Meregalli C (2021) Neuroinflammatory process involved in different preclinical models of chemotherapy-induced peripheral neuropathy. Frontiers in Immunol 11:1
11. Gangadharan V, Selvaraj D. Kurejova M, Njoo C, Gritsch S, Skoricova D et al. (2013) A novel biological role for the phospholipid lysophosphatidylinositol in nociceptive sensitization via activation of diverse G-protein signaling pathways in sensory neurons in vivo. Pain 154:2801–2812.
12. Guerrero-Alba R, Barragan-Iglesias P, Gonzalez-Hernandez A, Valdez-Morales E, Granado-Soto, Condes-Lara m, Rodriguez M, Marichal-Cancino B (2019) Some prospective alternative for treating pain: the endocannabinoid system and its putative receptors GPR18 and GPR55. Frontiers in Pharmacol 9:1–20.
13. Gutierrez-Gutierrez GM, Sereno, et al. (2010) Chemotherapy-induced peripheral neuropathy: clinical features, diagnosis, prevention and treatment strategies. Clin Transl Oncol 12 (2):81–91.

14. Han Y, Smith MT (2013) Pathobiology of cancer chemotherapy-induced peripheral neuropathy (CIPN). Frontiers in Pharmacol 4:156.
15. Iuchi K, Nishimaki K, Kamimura N, Ohta S (2019) Molecular hydrogen suppresses free-radical-induced cell death by mitigating fatty acid peroxidation and mitochondrial dysfunction. Can J Physiol Pharmacol 10:999–1005.
16. Jiang H, He H, Chen Y, Huang W, Cheng J et al. (2017) Identification of a selective and direct NLRP3 inhibitor to treat inflammatory disorders. J Exp Med 214:3219–3238.
17. Kelley N, Jeltema D, Duan Y, He Y (2019) The NLRP3 inflammasome: an overview of mechanisms of activation and regulation. Intl J Mol Sci 20: 3328.
18. Kinney WA, McDonnell ME, Zhong HM, Liu C, Yang L, Ling W, Qian T, Chen Y, Cai Z, Petkanas D, Brenneman DE (2016) Discovery of KLS-13019, a cannabidiol-derived neuroprotective agent, with improved potency, safety, and permeability. ACS Med Chem Lett 7:424–428.
19. Kodama D, Ono H, Tanabe M (2007) Altered hippocampal long-term potentiation after peripheral nerve injury in mice. Eur J Pharmacol 574: 127–132.
20. Krames ES (2014) The role of the dorsal root ganglion in the development of neuropathic pain. Pain Med 15:1669–1685.
21. Kurano M, Kobayashi T, Sakai E, Tsukamoto K, Yatomi Y (2021) Lysophosphatidylinositol, especially albumin-bound form, induces inflammatory cytokines in macrophages. FASEB J 35(6):e21672. doi: 10.1096/fj.202100245R.
22. LaPointe NE, Morfini G, Brady ST, Feinstein SC, Wilson L, Jordon MA (2013) Effects of eribulin, vincristine, paclitaxel and ixabepilone on fast axonal transport and kinesin-1 driven microtubule gliding: implication for chemotherapy-induced peripheral neuropathy. Neurotox 37: 231–239.
23. Li X, Wang L, Fang P, Sun Y, Jiang X, Wang H, Yang X-F (2018) Lysophospholipids induce innate immune transdifferentiation of endothelial cells, resulting in prolonged endothelial activation. J Biol Chem 293:11033–11045.
24. Milost J, Bryk M, Starowicz K. (2020) Cannabidiol for pain treatment: focus on pharmacology and mechanism of action. Intl J Mol Sci 21:8870.
25. Nezhady MAM, Rivera JC, Chemtob S (2020) Location bias as emerging paradigm in GPCR biology and drug discovery. iScience 23:101643.
26. Okine BN, Mc Laughlin G, Gaspar JC, Harhen B, Roche M, Finn DP (2020) Antinociceptive effects on the GPR55 antagonists CID16020046 injected into the rat anterior cingulate cortex. Neurosci 443:19–29.
27. Peters CM, Jimenez-Andrade JM, Jonas BM, Sevcik MA, Koewler NJ, Ghilardi JR, Wong GY, Mantyh PW (2007) Intravenous paclitaxel administration in the rat induces a peripheral sensory neuropathy characterized by macrophage infiltration and injury to sensory neurons and their supporting cells. Exp Neurol 203(1):42–54. https://doi: 10.1016/j.brainres.2007.06.066. Epub 2007 Jul 17.
28. Rajagopal S and Shenoy SK (2018) GPCR desensitization: acute and prolonged phases. Cell Signal 41:9–16.

29. Ryan D, Drysdale AJ, Lafourcade C, Pertwee RG, Platt B. (2009) Cannabidiol targets mitochondria to regulate intracellular Ca^{2+} levels. J Neurosci 29: 2053–2063.
30. Schuelert N, McDougall J (2011) The abnormal cannabidiol analogue O-1602 reduces nociception in a rat model of acute arthritis via the putative cannabinoid receptor GPR55. Neurosci Lett 500:72–76.
31. Smith JA, Slusher BS, Wozniak KM, Farah MH, Smiyun G. Wilson L, Feinstein S, Jordan MA (2016) Structural basis of induction of peripheral neuropathy by microtubule-targeting cancer drugs. Cancer Res 76:5115–5123.
32. Son S, Shim DW, Hwang I, Park JH Yu JW. (2019) Chemotherapeutic agent paclitaxel mediates priming of NLRP3 inflammasome activation. Front Immunol 10:1108.
33. Staff NP, Fehrenbacher JC, Caillaud M, Damaj MI, Segal RA, Rieger S. (2020) Pathogenesis of paclitaxel-induced peripheral neuropathy: a current view of in vitro and in vivo findings using rodent and human model systems. Exp Neurol 324: 113121.
34. Staton PC, Hatcher JP, Walker DJ, Morrison AD, Shapland EN, Hughes JP, Chong E, Mander PK et al. (2008) The putative cannabinoid receptor GPR55 plays a role in mechanical hyperalgesia associated with inflammatory and neuropathic pain. Pain 139: 225–236.
35. Suofu Y, Li W, Jean-Alphonse FG, Jia J, Khattar NK, Li J et al. (2017) Dual role of mitochondria in producing melatonin and driving GPCR signaling to block cytochrome c release. PNAS (USA) 114: E7997-E8006,
36. Tyrtyshnaia A, Manzhulo I. (2020) Neuropathic pain causes memory deficits and dendrite tree morphology changes in mouse hippocampus. J Pain Res 13:345–354.
37. Ward SJ, Ramirez MD, Neelakantan H, Walker EA (2011) Cannabidiol prevents the development of cold and mechanical allodynia in paclitaxel-treated female C57Bl6 mice. Anesth Analg 113: 947–950.
38. Ward SJ, McAllister SD, Kawamura R, Murase R, Neelakantan H, Walker EA (2014) Cannabidiol inhibits paclitaxel-induced neuropathic pain through 5-HT1A receptors without diminishing nervous system function or chemotherapy efficacy. Brit J Pharmacol 171: 636–645.
39. Ward SJ, Riggs D, Tuma R, Kinney WA, Petkanas D. Brenneman DE (2017) Neuroprotective and anti-inflammatory effects of KLS-13019 and cannabidiol in *in vitro* and *in vivo* models of chemotherapy-induced neuropathic pain. International Cannabinoid Research Society Symposium, June 22, 2017, Montreal, Canada, 27: P1-40.
40. Xu Z, Lv XA, Dai Q, Ge YQ, Xu J (2016) Acute upregulation of neuronal mitochondrial type-1 cannabinoid receptor and it's role in metabolic defects and neuronal apoptosis after TBI. Mol Brain 9:25.
41. Yamashita A, Oka S, Tanikawa T, Hayashi Y, Nemoto-Sasaki Y, Suigiura T (2013) The actions and metabolism of lysophosphatidylinositol, an endogenous agonist for GPR55. Prostaglandins and other Lipid Mediators 107: 103–116.
42. Zeng QZ, Yang F, Li CG, Xu LH, He XH et al. (2019) Paclitaxel enhances the innate immunity by promoting NLRP3 inflammasome activation in macrophages. Front Immunol 10:72.

Figures

Figure 1a

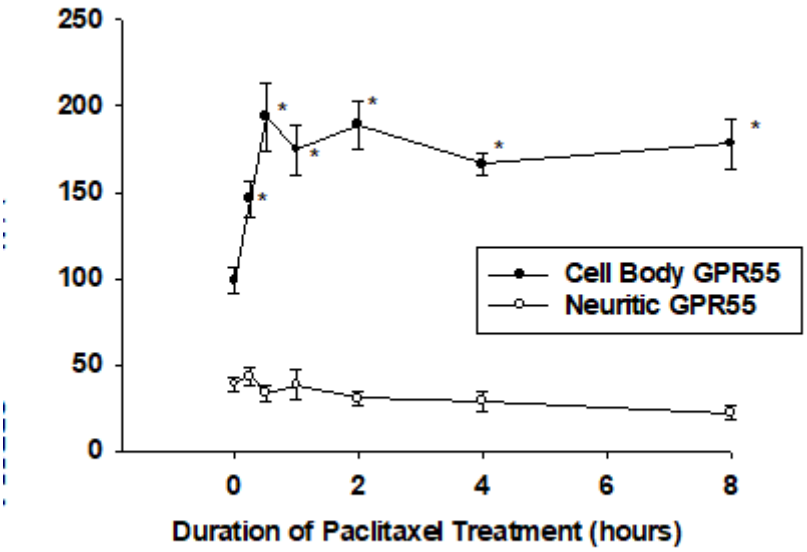

Figure 1b

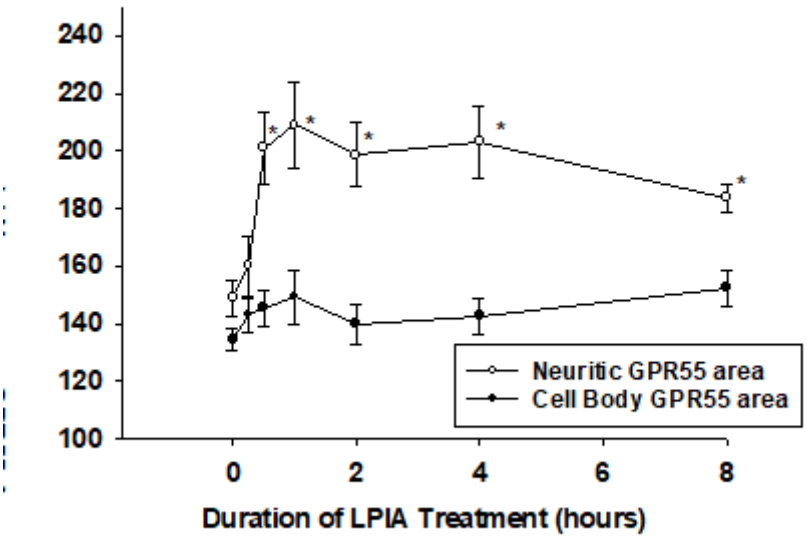

Figure 1

Figure 1a. The time course of paclitaxel-mediated effects on GPR55 immunoreactive (IR) area in cell bodies (closed circles) and neurites (open circles) of cultured DRG neurons were compared. All data were obtained from high content analyses of fluorescent neuronal images. * For cell bodies, significant

increases (P< 0.01) in GPR55 IR area from control levels were designated with an asterix. There were no significant changes in neuritic GPR55 IR area after paclitaxel treatment in comparison to controls. Each point is the mean value from 10 culture wells comprised of 20 fields (895 m x 895 m) per well from two replicate experiments. The error bars are the standard error. In **Figure 1b**, the time course of lysophosphatidylinositol arachidonate (LPIA)-mediated effects on GPR55 IR area in cell bodies (closed circles) and neurites (open circles) in DRG neurons were compared. All data were obtained from high content analyses of fluorescent neuronal images. *For neurites, significant increases (P< 0.01) in GPR55 area from control levels were designated with an asterix. There were no significant changes GPR55 area in the cell bodies of LPIA-stimulated DRG neurons. These data are the mean of six wells comprised of 20 fields each from a representative experiment. The error bars are the standard error.

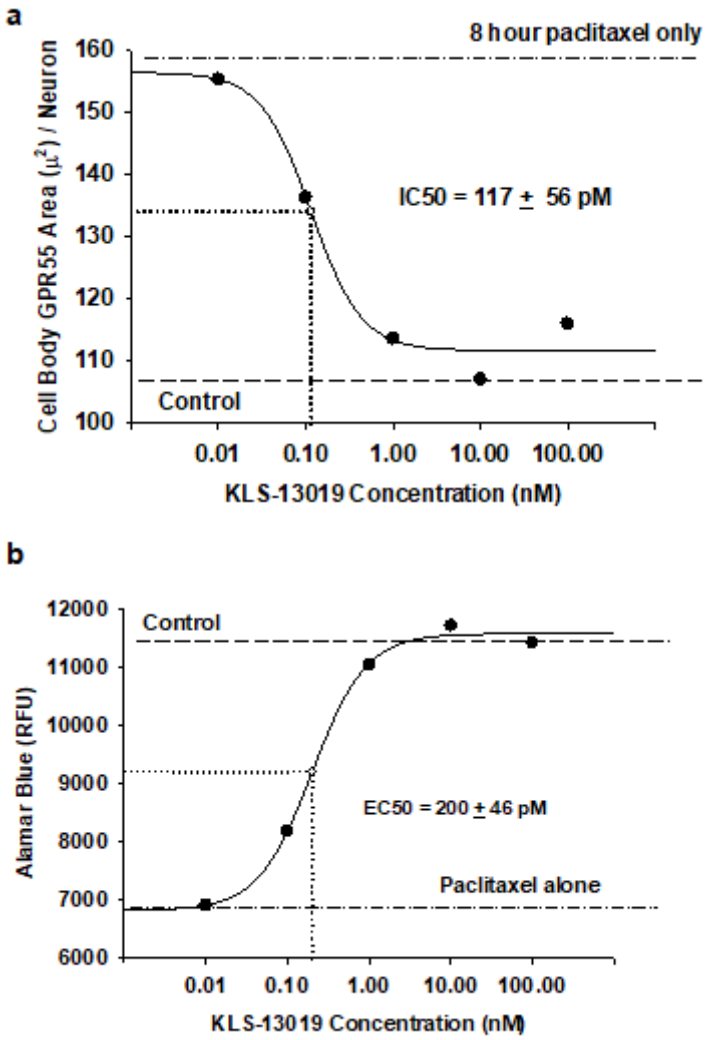

Figure 2

Figure 2a. The determination of the IC50 of KLS-13019 in decreasing paclitaxel-induced increases in cell body GPR55 IR area in DRG cultures as measured with high content fluorescence microimaging after a

reversal treatment paradigm: hours 0-24 with 3mM paclitaxel, inclusive of hours 8-24 treatment with various concentrations of KLS-13019. The reference line (dot-dash) indicates the mean cell body GPR55 area/neuron in cultures treated for 8 hours with paclitaxel alone, just prior to the addition of KLS-13019 for an additional 16 hours. The level of GPR55 area in control cultures is shown with the dashed reference line. Each point is the mean of 12 culture wells comprised of 20 fields from two replicate experiments. The standard errors of data points were ≤ 6% of the mean. The IC50 was determined from a 4-parameter logistic analysis. **Figure 2b.** Cell viability was measured with alamar blue using the same "reversal "treatment paradigm described above. The EC50 of increases in cell viability in DRG cultures are shown after treatment with KLS-13019 after a 24-hour treatment period. The reference lines indicated cultures responses of control (dashed line) and 8 hours treatment of paclitaxel (dot-dash) as in figure 2a. Each point is the mean of 6 determinations from a representative experiment. The standard error of each data point was ≤ 5-8 % of the mean. The EC50 was determined from a 4-parameter logistic analysis.

Figure 3a

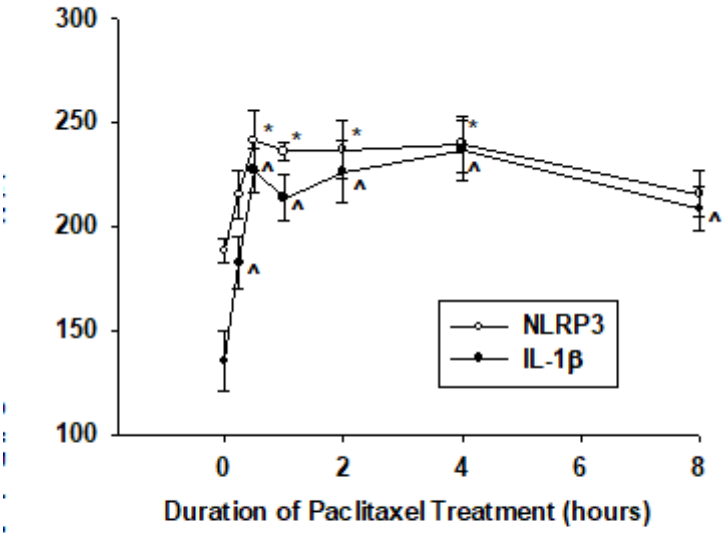

Figure 3b

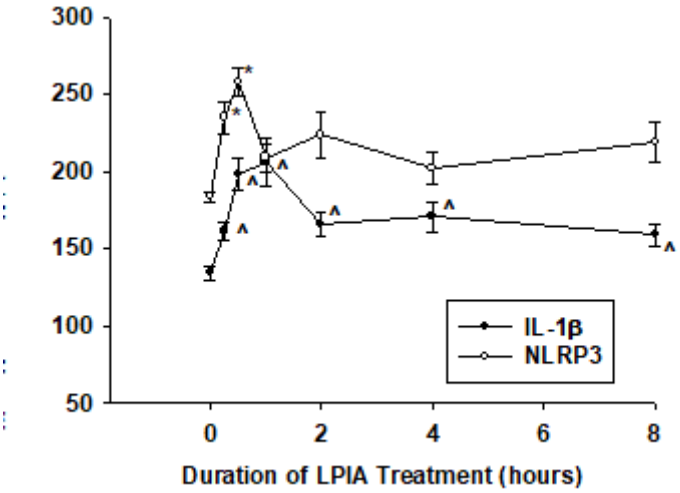

Figure 3

Figure 3a. The time course of paclitaxel-induced increases in IL-1b and NLRP3 IR areas in cell bodies of dissociated DRG cultures. All data were obtained from high content analyses of fluorescent neuronal images. *For NLRP3 (open circles), significant increases (P< 0.001) from control levels were observed from 30 min to 8 hours of 3 mM paclitaxel treatment. Each point is the mean of 6 well determinations obtained from 20 fields per well from replicate experiments. For IL-1**b** (closed circles), significant increases (P< 0.01) from control values were observed from 15 min to 8 hours of paclitaxel treatment as shown by the symbol: **^**. Each point is the mean of 10 well determinations from 20 fields per well from replicate experiments. **Figure 3b.** The time course of 1 nM lysophosphatidylinositol arachidonate (LPIA) treatment of DRG cultures. All data were obtained from high content analyses of fluorescent neuronal

images. *For neuritic NLRP3 IR area (open circles), significant increases (P< 0.01) from control levels were observed from 15 min to 30 min of 1nM LPIA treatment. Each point is the mean of 8 well determinations obtained from 20 fields per well from replicate experiments. ^ For neuritic IL-1b immunoreactive area (closed circles), significant increases (P< 0.01) from control values were observed from 15 min to 8 hours of paclitaxel treatment. Each point is the mean of 12 well determinations from 20 fields per well from replicate experiments.

Figure 4a

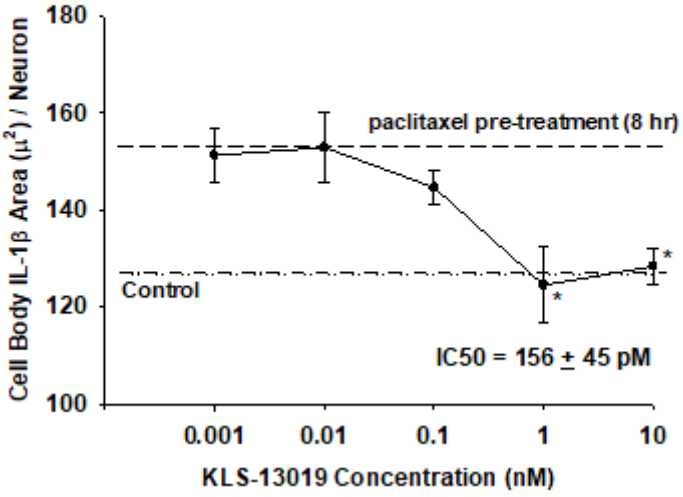

Figure 4b

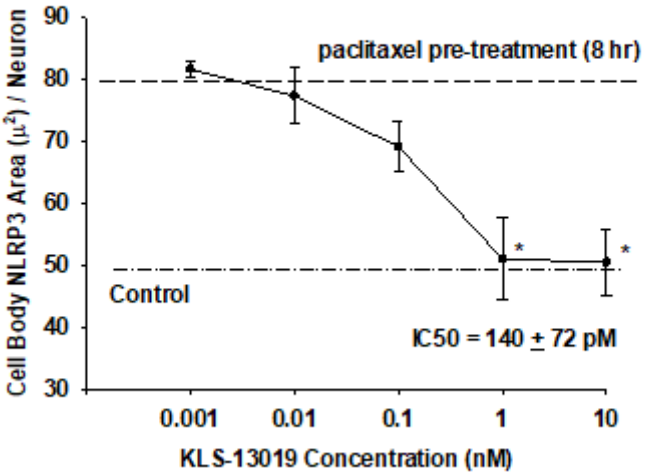

Figure 4

Figure 4a The effect of KLS-13019 in reversing paclitaxel-induced increases in cell body IL-1b IR area in dorsal root ganglion cultures during a 24-hour test period is shown. Increases in IL-1b were produced in 8-

hour incubations with 3 mM paclitaxel as shown by the dashed reference line. The cultures were then treated with various concentrations of KLS-13019 for an additional 16 hours without the removal of the paclitaxel. The cultures were then terminated for high content analyses of IL-1b IR area. Each data point is the mean of 6 well determinations comprised of 20 fields from a representative experiment. A references line (dot-dash) depicting the mean value of cell body IL-1b IR area for control DRG cultures is shown. **Figure 4b**. The effect of KLS-13019 in reversing paclitaxel-induced increases in cell body NLRP3 IR area in dorsal root ganglion cultures during a 24-hour test period. Increases in NLRP3 area were produced in 8-hour incubations with 3 mM paclitaxel as shown by the dashed reference line. The cultures were then treated with various concentrations of KLS-13019 for an additional 16 hours without the removal of the paclitaxel. The cultures were then terminated for high content analyses of NLRP3 IR area. Each data point is the mean of 6 well determinations comprised of 20 fields from a representative experiment. A references line (dot-dash) depicting the mean value of cell body NLRP3 IR area for control DRG cultures is shown. The error bars are the standard error.

Figure 5a

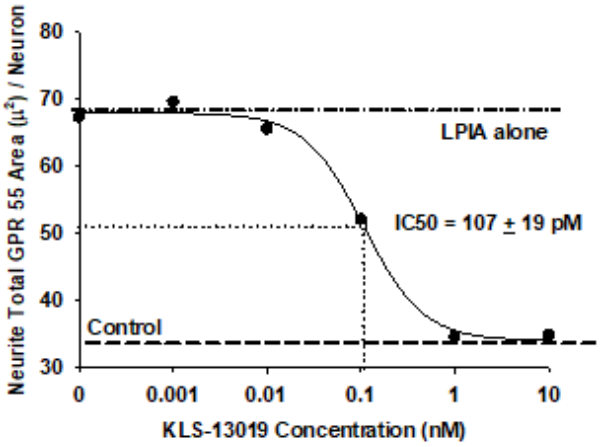

Figure 5c

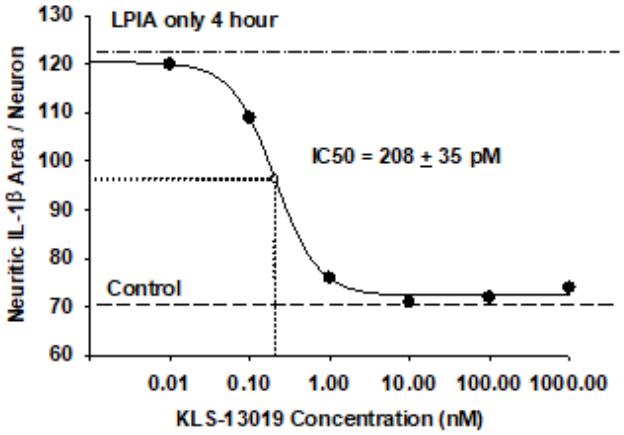

Figure 5b

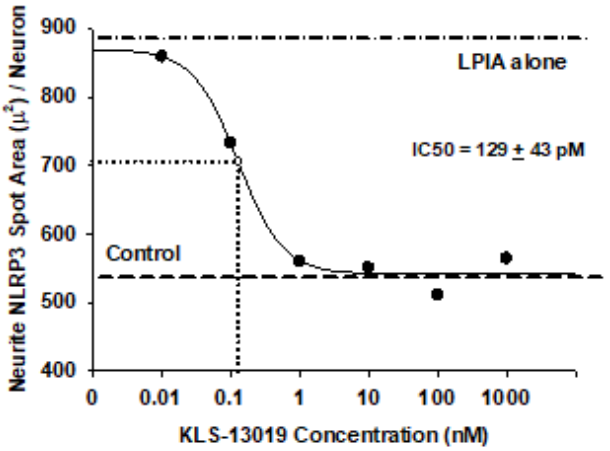

Figure 5d

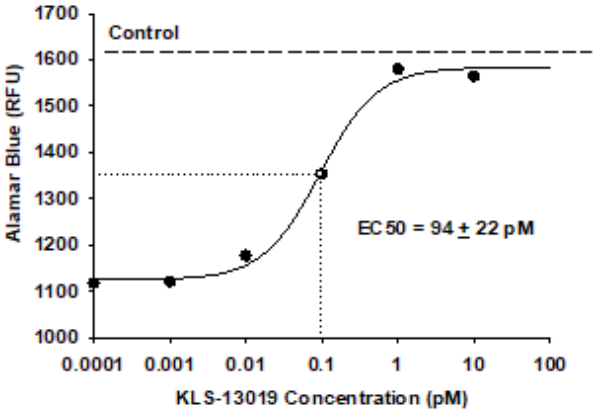

Figure 5

Figure 5a. The determination of the IC50 of KLS-13019 in decreasing LPIA-induced increases in neuritic GPR55 IR area in hippocampal cultures as measured with high content fluorescence microimaging after a reversal treatment paradigm: hours 0-4 with 1 nM LPIA alone followed by hours 4-8 treatment with various concentrations of KLS-13019. The reference line (dot-dash) indicates the mean neuritic GPR area/neuron in cultures treated for 4 hours with LPIA alone, just prior to the addition of KLS-13019 for an additional 4 hours. The level of GPR55 IR area in control cultures is shown with the dashed reference line. Each point is the mean of 8 determinations from 10 fields from a representative experiment of two replications. The standard error of each data point was ≤ 6-8 % of the mean. The IC50 was determined from a 4-parameter logistic analysis. **Figure 5b.** The determination of the IC50 of KLS-13019 in decreasing LPIA-induced increases in neuritic NLRP3 IR area in hippocampal cultures as measured with

high content fluorescence microimaging after a reversal treatment paradigm: hours 0-4 with 1 nM LPIA followed by hours 4-8 treatment with various concentrations of KLS-13019 is shown. The reference line (dot-dash) indicates the mean neuritic NLRP3 area/neuron in cultures treated for 4 hours with LPIA alone, just prior to the addition of KLS-13019 for an additional 4 hours. The level of NLRP3 area in control cultures is shown with the dashed reference line. Each point is the mean of 8 determinations from 10 fields from a representative experiment of two replicates. The standard error of each data point was $\leq$ 6-9 % of the mean. The IC50 was determined from a 4-parameter logistic analysis.

Figure 5c. The determination of the IC50 of KLS-13019 in decreasing LPIA-induced increases in neuritic IL-1b IR area in hippocampal cultures as measured with high content fluorescence microimaging after a reversal treatment paradigm: hours 0-4 with 1 nM LPIA followed by hours 4-8 treatment with various concentrations of KLS-13019 is shown. The reference line (dot-dash) indicates the mean neuritic IL-1b area/neuron in cultures treated for 4 hours with LPIA alone, just prior to the addition of KLS-13019 for an additional 4 hours. The level of IL-1b area in control cultures is shown with the dashed reference line. Each point is the mean of 8 determinations from 10 fields from a representative experiment from two replicate experiments. The standard error of each data point was $\leq$ 5-8% of the mean. The IC50 was determined from a 4-parameter logistic analysis.

Figure 5d. Cell viability was measured with alamar blue using the same “reversal “treatment program described above. The EC50 of increases in cell viability in DRG cultures are shown after treatment with KLS-13019 after the 8-hour treatment period. The reference lines indicated cultures responses of control (dashed line) and a 4-hour treatment with LIPA (dot-dash) alone to establish a cell viability response prior to treatment with KLS-13019. Each point is the mean of 8 determinations from a representative experiment. The standard error of each data point was $\leq$ 3-6 % of the mean. The EC50 was determined from a 4-parameter logistic analysis.

Figure 6a

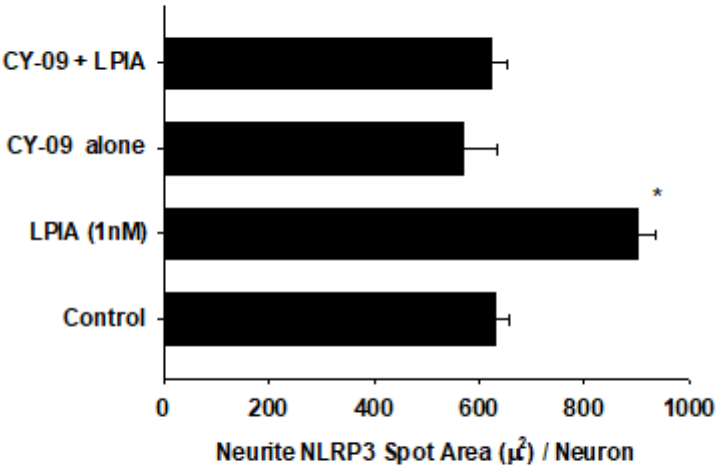

Figure 6b

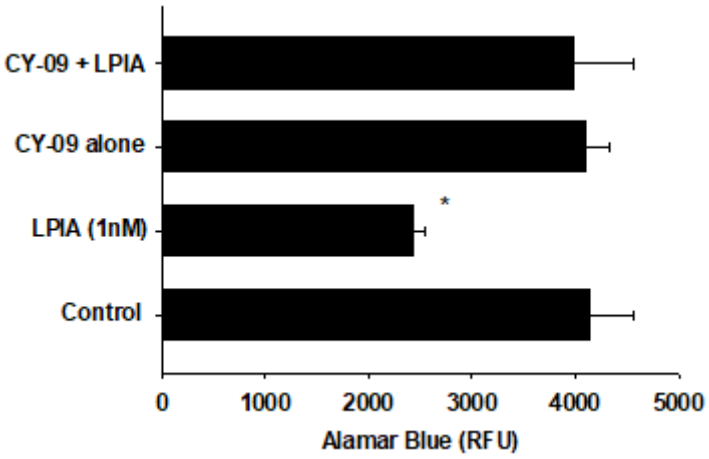

Figure 6

Figure 6a. The effect of the inflammasome-3 assembly inhibitor Cy-09 is shown on LPIA-mediated increases in NLRP3 in hippocampal cultures after 6 hours of treatment on day 16 in culture. Cultures were pre-treated with 10 mM CY-09 for 30 minutes prior to treatment with 1nM LPIA. At termination, cultures were fixed and analyzed by high content imaging of spot IR area for NLRP3 in neurons. Significant increases ($P< 0.001$) in neuritic NLRP3 area were observed in comparison to all other groups. Each bar is the mean of 8 well determination made from 10 fields per well from a representative experiment. The error bar is the SEM. **Figure 6b.** In the same cultures as utilized in 6A, prior to fixation for high content analysis, the cultures were assayed for cellular viability with alamar blue. Treatment with 1 nM LIPA produced a significant decrease in this viability assay that was 58 $\pm$ 3 %

of that observed for control. The LIPA-mediated decreases in cellular viability were prevented by pre-treatment with 10 mM CY09. Treatment with CY09 alone produced no significant difference from control.

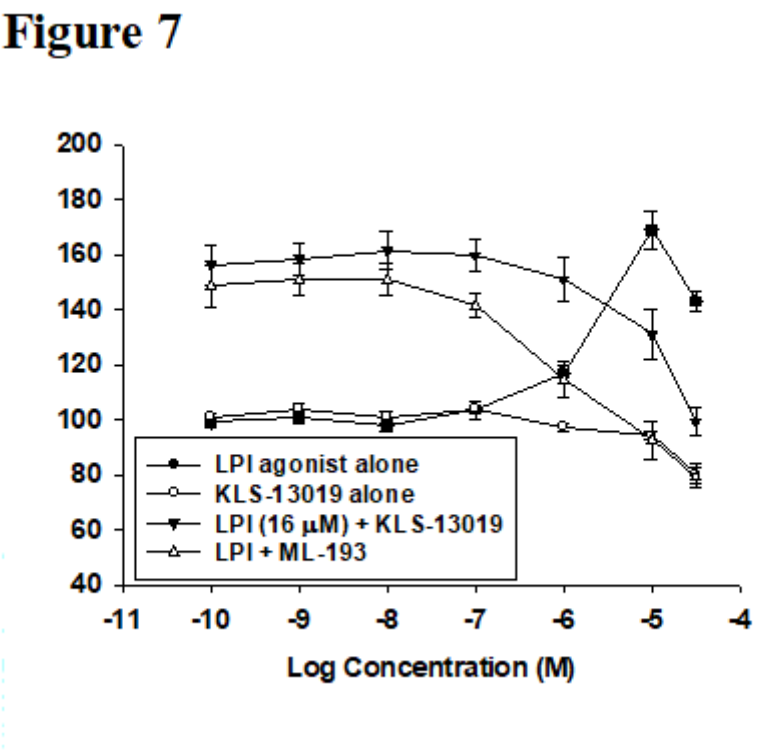

Figure 7

Figure 7. Evidence of human GPR55 antagonism by KLS-13019 was demonstrated with a DiscoverX assay from which increases in b-arrestin produced by 16 mM LPI were completely blocked by 30 mM KLS-13019 in this transfected model system. Dose response are compared for their activity in the b-arrestin assay: LPI alone (closed circles), KLS-13019 alone (open circles), LPI (16 mM) + KS-13019 (closed inverted triangles) and LPI (16 mM + ML-193 (open triangles). ML-193 is a known GPR55 antagonist (Kurano et al., 2021). Each point is the mean of 6 determinations in a representative experiment from duplicate studies. The error par is the standard error.

Figure 8

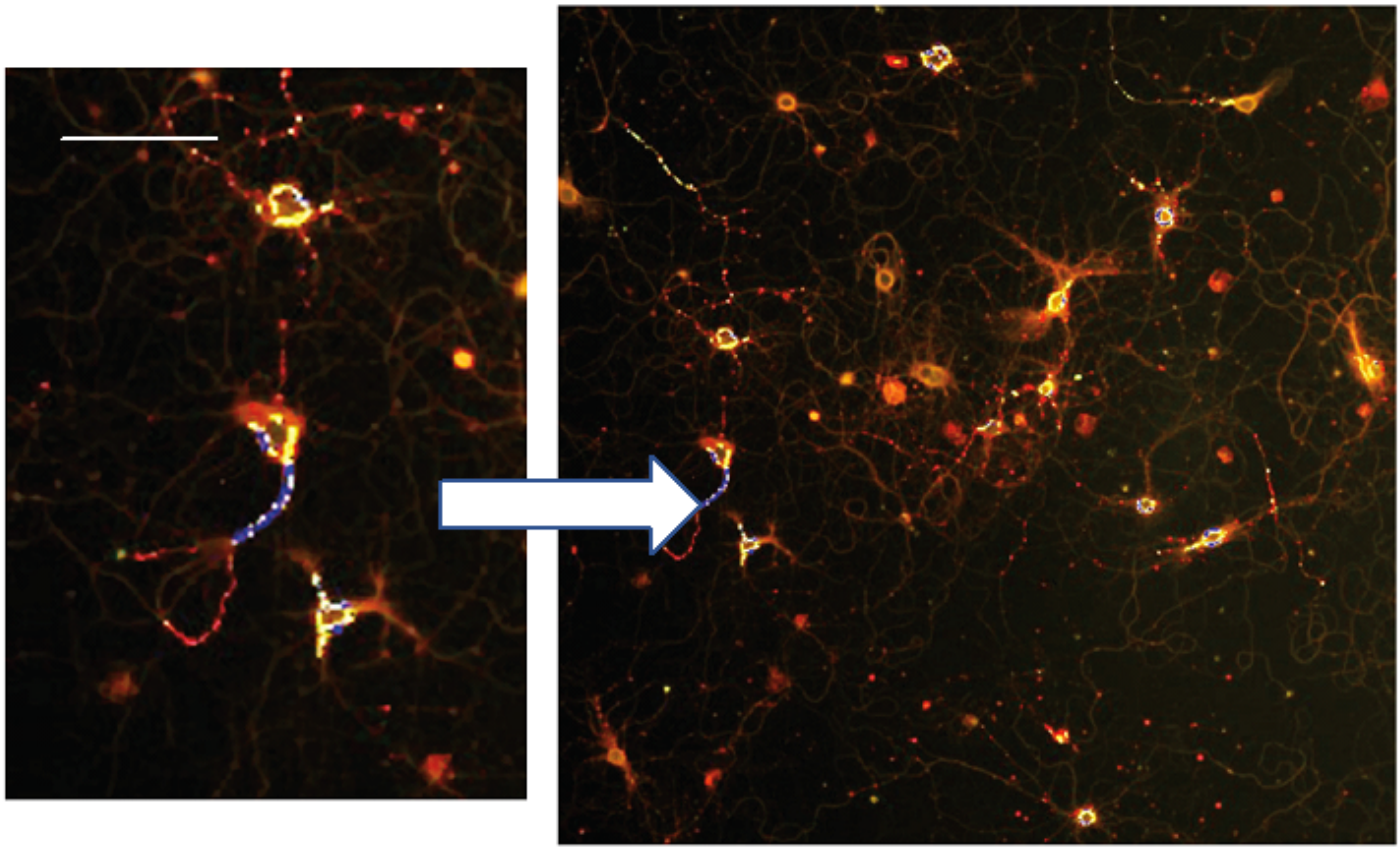

Figure 8

Figure 8. Immunofluorescence of GPR55 in day 21 hippocampal cultures as analyzed by a spot analysis from high content imaging after a 4-hour treatment with 1 nM LPIA. A spot co-localization algorithm within the neuronal profiling bioapplication was used to screen spot IR area for GPR55 and COX4 that were 100% overlapping. Identification of such co-localized spots were display utilizing pseudo color blue, with spots showing less than 100% overlap being displayed in red for GPR55 and yellow for COX4. A prominent area of blue spot overlap of GPR55 and COX4 on a proximal neurite is highlighted in left panel magnification of the high content imaging. The calibration bar is 20 µ.